



ELSEVIER

Journal of Photochemistry and Photobiology A: Chemistry 144 (2001) 13–19

Journal of  
Photochemistry  
and  
Photobiology  
A: Chemistry

www.elsevier.com/locate/jphotochem

# Excited state dynamics of oligothiophenes studied by transient pump-probe spectroscopy

G. Lanzani\*, G. Cerullo, S. Stagira, S. De Silvestri

*Istituto Nazionale per la Fisica della Materia, Dipartimento di Fisica, Politecnico di Milano, P. za L. da Vinci 32, 20133 Milano, Italy*

## Abstract

The primary excitations and their deactivation channels in oligothiophenes are discussed based on experimental results from time resolved spectroscopy with 200 fs time resolution. Molecules in solution and different morphology films are considered, in order to deduce the effect of molecular aggregation onto the nature of the excited states. A comprehensive interpretation of the rich phenomenology observed upon changing the aggregation state is proposed. © 2001 Elsevier Science B.V. All rights reserved.

**Keywords:** Oligothiophenes; Excitations; Transient spectroscopy

## 1. Introduction

Oligothiophenes ( $T_n$ ) were first isolated and synthesized in 1947 [1], but only recently they have been receiving the attention of a vast scientific community, due to their potential application in organic macroelectronics [2]. This emerging new field of applied science concerns the use of conjugated materials (i.e. containing carbon atoms and delocalized  $\pi$ -electrons) as semiconducting layers in thin film devices such as light emitting diodes, photodetectors, solar cells and so on. The  $T_n$  were first introduced as model compounds for the longer chain, polymer counterpart. It was then reckoned that these materials possess very interesting properties on their own and can be used for realization of devices. Thin film field effect transistors, which were first built using  $T_6$  in 1990 [3,4], have nowadays reached performances, in terms of carrier mobility and on/off ratios that are close to market applications [5]. There existing review papers on the subject [6,7], which comprises synthesis, and growth, optical and electrical properties of  $T_n$ , lack a comprehensive discussion on the electronic states dynamics and deactivation mechanisms. The identification of the primary excitations supported by these materials and of their evolution are of primary importance for a thorough understanding of their opto-electronic properties and for this reason transient phenomena have been extensively investigated by using a variety of time resolved spectroscopy techniques. There exists a rich topical literature on this subject.

In this paper, we will report about our recent results concerning excited state dynamics of  $T_n$  in different aggregation states. We will focus our attention on transient spectroscopy, in particular on pump-probe experiments. The discussion will also concern published data for solution, films and single crystals obtained by other groups, in order to provide a broad and comparative view of the photophysics of  $T_n$  depending on the inter-molecular interactions. However, note that a comprehensive review of the subject goes beyond the scope of this work, which is intended to be a brief account of the state of the research. Finally, we note that highly pure single crystals of organic semiconductors, recently obtained by Schön and co-workers [8,9], have shown exceptional properties [10], remarking the value of such samples for exploring fundamental issues. Single crystals, however, may not be so advantageous for applications as compared to thin films, which thus deserve to be the object of a deep investigation.

## 2. Experimental

The samples under study, whose chemical structure is shown in Fig. 1, are solution of diethyl-quinquethiophene ( $T_5A$ ), highly ordered polycrystalline films  $\alpha\omega$ -dihexyl-sexithiophene ( $\alpha\omega T_6$ ) and amorphous films of non regioregular  $\beta,\beta'$ -dihexyl-sexithiophene ( $\beta T_6$ ). The oligomers were synthesized as described in [11,12]. The  $T_5A$  was chosen for its high solubility in most organic solvents. Solution were prepared in THF at concentration of about  $10^{-4}$  M. Thin films were prepared by evaporation under reduced pressure of the powdered compound on glass substrates. Structural

\* Corresponding author. Tel.: +392-267-47-11; fax: +392-239-061-26.

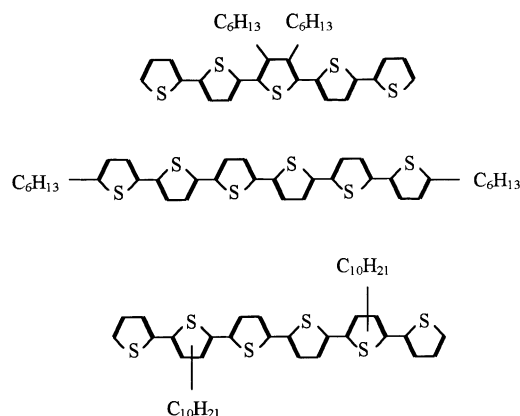


Fig. 1. Chemical structure of the thiophene derivatives used in this work.

characterization as well as optical and electrical properties have been studied elsewhere [13]. For  $\beta T_6$ , no clear structural organization could be deduced from X-ray diffraction analysis as a consequence of the positional disorder caused by the non-regioregular substitution. Based on general considerations on packing of the analog stereo-regular compound we expect the formation of disordered one dimensional clusters (stacks) with variable lengths in which the randomly placed molecules are about 6 Å apart.

Polycrystalline films of  $\alpha\omega T_6$ , 0.1  $\mu\text{m}$  thick were deposited by vacuum evaporation at about 350°C and standard pressure conditions [11]. The chemical purity of the powder compound, after several sublimations, was  $10^{16} \text{ cm}^{-3}$ . The  $\theta$ - $2\theta$  X-ray diffraction spectrum [11] of a thick (few microns)  $\alpha\omega T_6$  film consists of a series of very sharp peaks that demonstrate the high degree of crystallinity that is obtained. Nanocrystals have monoclinic arrangement with unit cell parameters  $a = 5.88 \text{ \AA}$ ,  $b = 7.88 \text{ \AA}$  and  $c = 71.2 \text{ \AA}$ , and  $\beta = 111.3^\circ$ . The  $T_6$  moieties and the hexyl chains are segregated into spatially ordered homogeneous microdomains, which give rise to the multilayer structure. The X-ray pole figure characterization shows that only one spatial orientation is obtained corresponding to nanocrystalline domains (with 10–10<sup>3</sup> nm diameter) standing on the (a, b) plane parallel to the substrate. The  $\alpha\omega T_6$  molecules stand up on the substrate, closely packed in the herringbone geometry with minimum distance of 4.79 Å. Conductivity in  $\alpha\omega T_6$  films is highly anisotropic (a factor 10<sup>2</sup> in favor of the in plane direction), confirming the long range order of the stacking geometry.

The experimental set-up for pump-probe measurements is based on an amplified Ti-sapphire laser system and was described in detail elsewhere [14]. The excitation pulse at 3.18 eV, with 180 fs duration, was focussed to a spot size of 80  $\mu\text{m}$  and the excitation energy was varied from 20 to 250 nJ per pulse. Pump-probe experiments were carried out in the visible and near infrared spectral ranges using the white light supercontinuum generated by focusing the fundamental beam in a thin sapphire plate. Mirrors were used

to collect the supercontinuum pulse and to focus it on the sample in order to minimize frequency chirp effects. Two measurements were carried out: (i) the whole white light pulse was spectrally analyzed after traveling through the sample using a monochromator and a silicon diode array. Transmission difference spectra were obtained by subtracting pump-on and pump-off data measured in the 2.69–1.65 and 1.57–1.3 eV energy ranges. (ii) Temporal evolution of the differential transmission was recorded at selected wavelengths using a standard lock-in technique. The time resolution of the system was about 200 fs. In both experiments, the pump beam was linearly polarized at the magic angle with respect to the probe. For photoinduced anisotropy decay measurements the pump and probe polarization were set at 45° and an analyzer was placed behind the sample.

### 3. Results

#### 3.1. $T_5A$ in solution

In Fig. 2, we show the evolution of the transient transmission ( $\Delta T/T$ ) spectra of  $T_5A$  in THF solution after optical excitation at 3.2 eV. At short pump-probe delays the spectrum shows a positive  $\Delta T$  band at 2.4 eV, coincident with the photoluminescence peak, assigned to stimulated emission (SE), and a negative  $\Delta T$  band, due to photoinduced absorption (PA). After correction for spectral overlap with the second PA band (see below), these two features have identical decay kinetics, as shown in the inset of Fig. 2, indicating a mono-exponential time-constant of 308 ps. The decay of PA and SE is associated to the formation of a new PA band, centered at 1.95 eV, according to parent-son relation.

#### 3.2. $\beta T_6$ films

Fig. 3 shows  $\Delta T/T$  spectra of  $\beta T_6$  films at liquid nitrogen temperature for varying pump-probe delays ( $\tau_D$ ) and excitation density of  $10^{20} \text{ cm}^{-3}$  at 3.2 eV. For  $\tau_D = 0.4 \text{ ps}$ , we see two PA bands at 1.3 and about 1.6 eV (right where the Ti:sapphire laser fundamental radiation is, thus, limiting its detection). The spectrum turns positive at about 1.82 eV and shows three bands at 2, 2.4 and 2.6 eV. The  $\Delta T/T$  spectrum changes shape during time, the decay of PA around 1.6 eV is slower, and it is the only feature still present for  $\tau_D = 400 \text{ ps}$ . In the positive  $\Delta T$  region, the bands at 2.4 and 2.6 eV show initial fast decay followed by partial recovery. The same non-exponential kinetics, with a fast (about 1 ps) and a slow (hundreds of ps) decay component, is seen everywhere. Around 1.6 eV, however, the fast component is reduced. The positive peaks at 2.4 and 2.6 eV correspond to the first and second vibronic replica of the ground state absorption spectrum and can be assigned to photobleaching (PB). The positive band detected for wavelength longer than 2 eV falls in the region of photoluminescence and can be ascribed to SE.

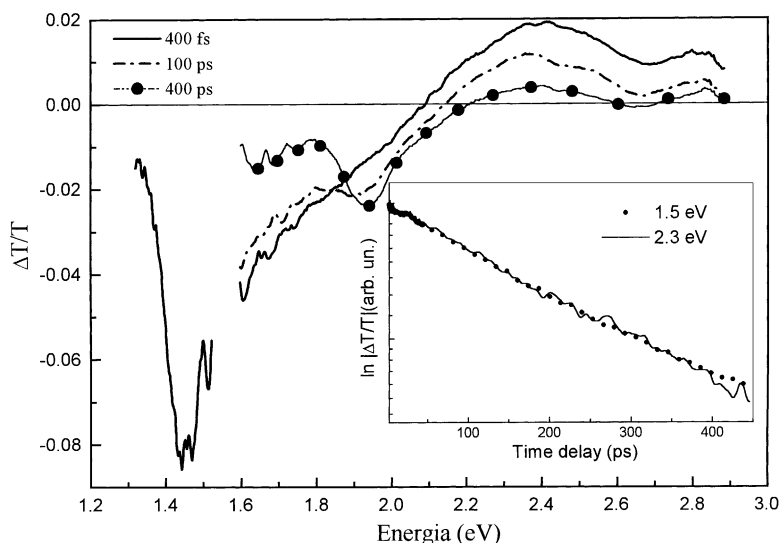


Fig. 2.  $\Delta T/T$  spectra at different pump-probe delays after excitation at 3.2 eV in  $T_5A$  in solution. The inset shows on a semi-log plot the decay kinetics of PA at 1.5 eV and SE at 2.3 eV, after correction for spectral overlap with PA at 1.95 eV.

### 3.3. $\alpha\omega T_6$ films

The most striking characteristic of  $\alpha\omega T_6$   $\Delta T/T$  spectrum (Fig. 4) is the lack of PB and SE at  $\tau_D = 0.4$  ps. There is a PA band at 1.6 eV while in the near IR region of the spectrum we can guess a PA band peaking outside the experimental range whose tail, indicated by the arrows in the plot, extends to the visible. The inset in Fig. 4 shows that the decay rate of PA at 1.8 eV is faster at higher excitation density. The intensity dependence is common to the whole spectrum, except

for the narrow region around 1.5 eV, thus, reflecting a dominant recombination mechanism in  $\alpha\omega T_6$  nano-crystals. The kinetics can be reproduced by a time-dependent bimolecular rate coefficient, linked to a reduction in time of the annihilation probability [15]. Note that in  $\beta T_6$  only monomolecular decay could be detected, in spite of the similar excitation conditions. Once recombination by exciton–exciton collision is concluded, PA decays as first-order kinetics with time constant of 30 ps. The decay of PA leads to a dramatic change of the  $\Delta T/T$  spectrum in which PB becomes evident.

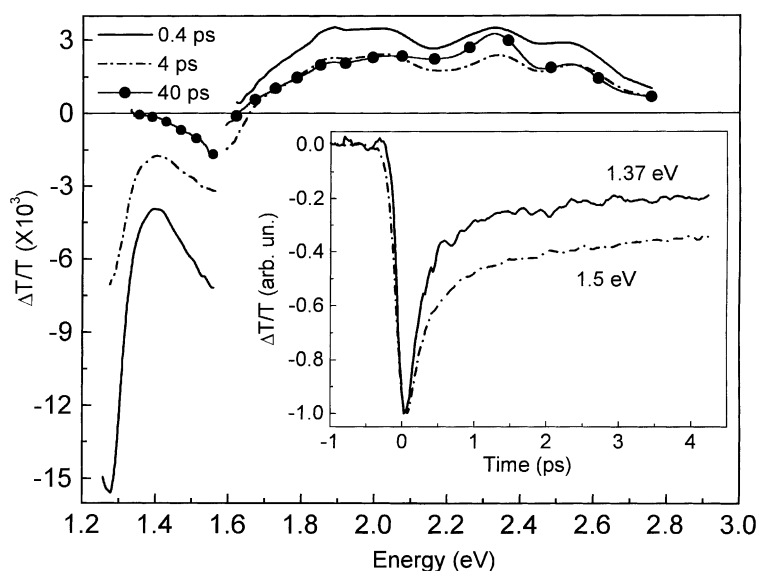


Fig. 3.  $\Delta T/T$  spectra at different pump-probe delays ( $\tau_D$ ) after excitation at 3.2 eV in  $\beta T_6$  films at 77 K. Up to 400 ps, the spectrum do not show any detectable change. The inset shows the decay kinetics at 1.5 and 1.37 eV.

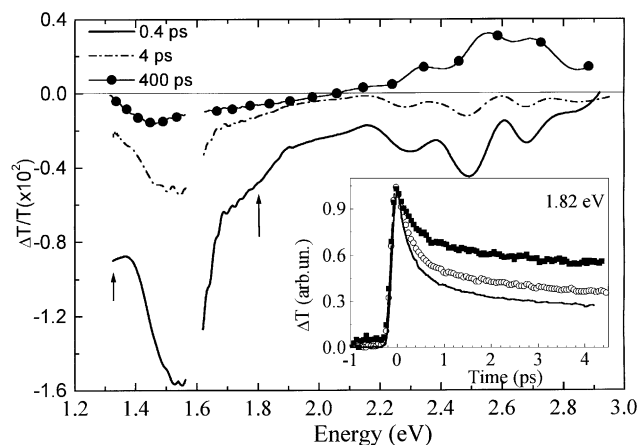


Fig. 4.  $\Delta T/T$  spectra at different pump-probe delays ( $\tau_D$ ) after excitation at 3.2 eV in  $\alpha\omega T_6$  films at 77 K. The inset shows intensity dependent kinetics at 1.82 eV for excitation density of: solid line  $3 \times 10^{20} \text{ cm}^{-3}$ ; open circles  $1 \times 10^{20} \text{ cm}^{-3}$ ; closed squares  $5 \times 10^{19} \text{ cm}^{-3}$ .

## 4. Discussion

### 4.1. The isolated molecule

Charra et al. [16] and Chosrovian et al. [17] reported the first transient transmission difference spectra of  $T_n$  in solution in 1992, almost simultaneously. The spectra showed stimulated emission (SE) and photoinduced absorption (PA) bands with similar decay kinetics, thus, allowing a first assignment of the singlet–singlet  $S_1$ – $S_n$  transition energy and lifetime. For short  $T_n$  ( $n < 8$ ) a linear dependence of the transition energy on the inverse molecular size is found, i.e. a red shift for longer chains, according to the prediction of the simple free electron molecular orbital model [18]. The lifetime of the lowest excited state increases upon lengthening of the chain, from 45 ps for  $n = 2$  to 850 ps for  $n = 6$ , a phenomenon initially ascribed to chain-end effects [19]. The work done in solution clearly demonstrated that the lowest excited singlet state in  $T_n$  is optically allowed and responsible for emission and optical gain. More recent work done on substituted molecules [20–22] added information on the initial intra-band relaxation following photoexcitation, pointing out the role of geometrical relaxation. The  $T_n$  are not planar in their ground state when in solution, especially if side groups are attached to the main chain. In the excited state, however, their conformational mobility, particularly the inter-ring torsion, is much reduced, leading to planarization and stiffening of the backbone. This process has been observed as a red-shift of SE and fluorescence during the first ps after photoexcitation [20–22]. The process provides a good explanation for the weak solvent dependence of the  $T_n$  optical properties: stiffening of the molecular backbone freezes out the low energy motion (ring torsion) which is responsible for solute–solvent interactions. In addition planarization may control the branching ratio of non-radiative

versus radiative deactivation, through the subtle interplay between geometry, energy levels ordering and potential energy surfaces intercepts. This idea was recently developed to explain intersystem crossing in terthiophene [23].

We interpret the early steps of photoexcitation in  $T_5A$  as follows. After absorption at 3.2 eV fast thermalization brings the population down to the lowest singlet excited state,  $S_1$ . This is accompanied by nuclear adjustment, which re-normalizes the dimerization pattern and leads to a more planar geometry, within about 5 ps [24]. The increased conjugation of the planar structure is associated to a longer effective conjugation length, and a corresponding red shift of the SE spectrum is detected, as shown in Fig. 5. At longer delays SE and PA in the  $\Delta T/T$  are due to transitions originating from this “flat”, thermalized  $S_1$  state, i.e. to  $S_1 \rightarrow S_0$  and  $S_1 \rightarrow S_n$  transitions, respectively, in agreement with the common decay kinetic displayed in the inset of Fig. 2. There are three deactivation channels for  $S_1$  accounting for the observed lifetime of about 300 ps: (i) radiative decay (PL), associated to the same transition responsible for optical gain. (ii) Inter system crossing (ISC) identified by the long-lived triplet–triplet PA band at 1.95 eV. (iii) Internal conversion. Quantum efficiency measurements show that PL depletes about 10% of the excited state population. A rough evaluation of ISC efficiency, which over-estimates the real value, assumes equal cross-section for singlet and triplet transitions yielding about 30%. Internal conversion ( $S_1 \rightarrow S_0$ ) should, thus, take place with an efficiency exceeding 50%, in contrast with unsubstituted  $T_n$  for which it is almost negligible [25]. The decay kinetics of  $S_1$  in solution is fairly well described by a single exponential for both substituted and non-substituted molecules. However, we find that the time constant in the former is shorter than in the later (about 300 ps for  $T_5A$  against 850 ps for  $T_5$ ). This observation and the fact that the effective conjugation length is the same, as detected by the spectral position of PL and PA, requires to go beyond a simple chain-end-effect to explain the observed

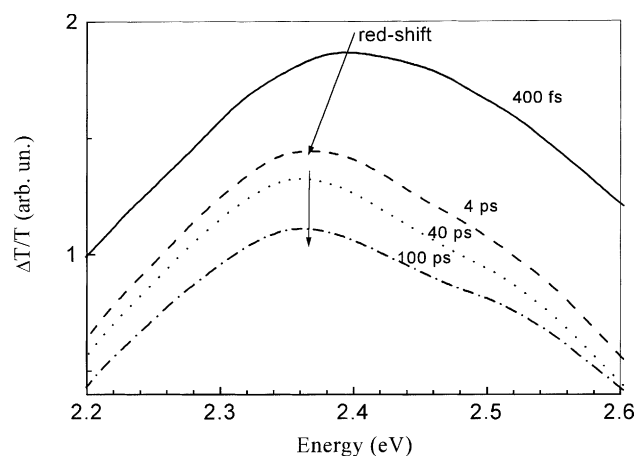


Fig. 5. Spectral migration of SE in  $T_5A$  solution in THF after photoexcitation at 3.2 eV at different pump-probe delays.

size-dependence in the decay kinetics. It is the overall stability of the planar state with respect to torsional deactivation that determines the lifetime of the state and its emission efficiency. Substitution introduces steric hinderance among the side groups which de-stabilized the planar configuration increasing the overall energy. Redistribution of the energy among low energy torsional modes becomes an efficient radiationless path to the ground state.

#### 4.2. The condensed phase

All in all the photophysics of  $T_n$  in solution is quite well understood, and the results in  $T_5A$  can be considered as a good starting point for discussing the much more involved situation of solid-state.<sup>1</sup> In solids, new decay channels open up, due to intermolecular interactions, defects and impurities. The molecular organization at nanoscopic level plays a fundamental role, because it can affect both the nature and the deactivation mechanism of the excited states. In particular, the periodic interaction between the molecules in the ordered structure induces the formation of collective excited states (Frenkel exciton), having different properties with respect to the isolated molecule states.

Before discussing the film properties, we would like to briefly describe recent reports about excited state dynamics in sexithiophene single crystals. These results are particularly instructive, because they allow identifying the fundamental, intrinsic excitation of  $T_6$  free from defect and impurity effects. The excited state transmission of  $T_6$  single crystal [26,27] shows a sharp PA band at 1.25–1.3 eV with asymmetric line-shape extending to the visible, up to 2 eV, possibly due to vibrational progression. This band is assigned to optical transitions starting from the lowest Frenkel exciton state of forbidden dipole character originated by Davydov splitting of the lowest lying singlet molecular state. Its energy location is close to that of the isolated molecule [16] as a consequence of the weak interactions in the crystal. The PA band decays non-exponentially within 2 ns, while a second PA band is formed, at 1.6 eV. The latter is long lived, being still observed in the  $\mu s$  time domain. The identification of this state is controversial: Klein assigns it to triplet–triplet transitions [27] while Frolov et al. to exciton trapped at defects [27].

We have described two very different cases, isolated molecules in solution and strongly interacting molecules in a crystal lattice. Based on these two extremes, we will now try to understand the properties of films. Polycrystalline films are a combination of nano-crystals that should in principle display the same properties of the isolated single crystal. The results in single crystal should thus find a correspondence in polycrystalline films. The latter, however, contain many trapping sites at the grain boundaries, where dislocation, local aggregation and defects can easily occur,

even in the best case of highly pure starting materials. This implies that it is difficult to distinguish the fundamental properties from those due to disorder. On the other hand, films are more attractive for technology application and disorder can be even useful for such effects as charge separation, which play a role in devices. For this reason we feel important to investigate disordered thin films in details.

##### 4.2.1. $\beta T_6$ films

Excitons should not be formed in the disordered structure of  $\beta T_6$  films, so we think more reasonable to assign  $S_1$  to a localized excitation with *molecular character*. Consequently, the PA band at 1.3 eV in  $\beta T_6$  should be compared to the one observed in  $T_5A$  in solution. The ultrafast decay dynamics, however, is in stark contrast to the single molecule: it is much faster, by three orders of magnitude and highly non-exponential. Bi-molecular recombination is ruled out by the lack of excitation intensity dependence [28]. Clearly the closeness of other molecules opens up a new, efficient decay channel, that's not available in solution. This is a first solid-state effect, upon passing from the solution to the film. In a previous work, it was proposed to assign it to generation of correlated polarons ( $T_6^+/P^-$ ) bound by Coulomb attraction: either closely lying oppositely charged pairs or positive radicals resulting from ionization at an impurity (e.g. oxygen) [28]. A second solid-state effect is the appearing, from the very beginning, of the PA band at 1.6 eV with different dynamics. The fast decay seen in the inset of Fig. 3 can be attributed to be spectral overlap, while the PA does not change in time, till 400 ps. Is this the same band observed in single crystals? Due to an incidental overlap of spectroscopic features in this region, it is difficult to answer the question. Looking for a simple model we assume it is. Let's call this state X-state. It could be a charge transfer (CT) excitation, as previously invoked for  $T_6$  [29], formed at particular sites of the clusters where for instance two  $\beta T_6$  molecules are face-to-face. This assignment is not fully alternative to that of triplet, because the CT state is doomed to decay quickly by geminate recombination, but during its lifetime may undergo inter system crossing, thus, surviving a long time as triplet state. Unfortunately spectroscopy can not distinguish between triplets and polarons in  $T_6$ , because both species absorb in the same region. We can, however, put forward some qualitative considerations. The X-state PA appears within the time resolution of our set-up. Being cautious due to the spectral overlap in the region, we can assume that the formation time constant is about 150 fs and the process completed in about 500 fs. During this time a fraction of singlets could decay into triplets. However, the measured (ISC) time, a measure of the probability for spin flip, is reported to be about 1.4 ns in  $T_6$  isolated molecule [25]. This implies that the fraction of spin-flip events in 150 fs is  $1 \times 10^{-4}$ . For a such tiny fraction of excitations to be detectable in our  $\Delta T/T$  spectrum we would need a triplet–triplet transition cross-sections 3–4 order of magnitude larger than that for singlet–singlet transitions, some-

<sup>1</sup> The results obtained are qualitatively unchanged for longer  $n$ , and can thus be used to compare with  $T_6$  in solid.

thing not justified at all. Based on dynamics and time scales arguments, it is thus rather unlikely that triplet be formed by the usual spin-flip molecular mechanism. Hot singlets may, however, have other channels for triplet conversion. There are three candidates that can be considered: (i) singlet exciton fission into triplet pairs; (ii) fusion and fission; (iii) charge carrier (or doublets) recombination. Here, (i) requires excitation energy at least equal to twice the triplet energy. In  $T_6$ , the  $S_0$ – $T_1$  gap is located between 1.5 and 1.58 eV, which are the phosphorescence energies for polythiophene and  $T_5$ , respectively [30]. However, in a previous work, we have shown that excitation at 2.3 eV gives similar results as those described here [29]. In addition, no magnetic field dependence was found in  $T_6$  fluorescence [31]. This argues against fission. (ii) Singlet fusion and fission from a higher lying state is excluded by the linear dependence on intensity of the PA. (iii) Charge separation and recombination within 500 fs is questionable, even if not impossible [32]. Being this the case, the process would be faster in a perfect crystals, contrary to the observations. All these cast doubt on X-PA be due to triplet–triplet transition, at least at the very beginning. We thus prefer the interpretation of the X-state as localized excitation: excimer, dimer or CT. This aggregate could be a defect in the single-crystal lattice. Localized distorted environments are actually often invoked to explain other  $T_n$  properties, such as luminescence [33,34].

#### 4.2.2. $\alpha\omega T_6$ films

The large separation between molecular layers allows considering  $\alpha\omega T_6$  as two-dimensional nanocrystals. Within one layer molecules are arranged in a rectangular lattice which is obtained as projection of the monoclinic lattice. There are two non-equivalent molecules per unit cell, so that the optically allowed intramolecular state splits in the crystal in two exciton bands (Davydov splitting) [35]. The lower lying band has small oscillator strength, in analogy to what occurs in the three-dimensional lattice, due to the anti-symmetric combination of the dipole moments of the molecular transitions. The high lying exciton component is optically allowed, with negative mass. As a consequence the model predicts that absorption in the crystalline phase, associated to transitions to the higher Davydov component, is blue shifted with respect to the intramolecular transition and that emission is red-shifted, and strongly suppressed. Several estimates of the Davydov splitting have been proposed. A crude evaluation, based on the so-called H-aggregate [36], set the Davydov splitting at 1 eV. Using the point dipole approximation and considering the geometry of the two-dimensional lattice a smaller value of 0.7 eV was found [37]. A smaller value of the Davydov splitting, of about 0.3 eV, has been proposed by Muccini et al. [38] based on high-resolution polarized spectra of  $T_6$  single crystals and confirmed by Frolov et al. [26]. This value has been extracted by inspection of the complex vibronic structure and it is supported by quantum mechanical calculations on small clusters.

The  $S_1$ – $S_n$  transition could not be directly detected in  $\alpha\omega T_6$ , but there is clear evidence of a band peaking just out of our experimental range ( $\sim 1.2$  eV). In addition, the bump at 1.8 eV (signed by an arrow in Fig. 4) is associated to this near infrared band. We assigned it to transitions from the dark exciton state to higher lying states, corresponding to the single crystal PA band. Again we observed the X-band at 1.6 eV, similar to the case of  $T_6$  [29] an  $\beta T_6$ . Frolov et al. [26] suggested that the instantaneous appearing of the X-band in defected systems is due to a very short trapping time, thus, assuming it has the very same nature of the state observed in single crystals. Possibly boundary regions separating the nanocrystals in  $\alpha\omega T_6$  films are source of such defects. Intensity dependent dynamics is clearly observed in  $\alpha\omega T_6$  at 1.8 eV, but not at 1.5–1.6 eV. This further demonstrates that the two states have different origin, and marks a difference with the molecular state dynamics of solution and  $\beta T_6$  films, always monomolecular. Once the exciton–exciton annihilation is concluded, we deduce slower recombination kinetics with 30 ps time constant, which is associated to the formation of PB. The initial lack of PB and its delayed formation can be assumed as further evidence for the presence of a low-cross-section (dark) transition at the band edge, consistently to the conjecture of a dipole forbidden exciton state. The initial spectrum would result from the overlap between PA, due to a higher energy exciton transition, and PB, with the former overwhelming the later. Once the PA is decayed, PB becomes visible.

In this discussion regarding the early events after photoexcitation, charged states do not appear to be important, except for the uncertain nature of the X-state. However, at long times (in the  $\mu s$  time domain) double charged states do appear in  $\alpha\omega T_6$  films following photoexcitation [39]. We conjecture that the X-state separates into charged species that further interact one another to give rise to long lived doubly charged states, as evidenced by steady-state photo-modulation experiments [39].

## 5. Conclusions

In this paper, we discussed the nature and deactivation channels of the primary excitations in  $T_n$ , as they can be deduced for time resolved spectroscopy. The “isolated” molecule in solution, a substituted pentamer, is described within the standard molecular picture, once geometrical relaxation associated to inter-ring twisting is taken into account. We suggest that torsional deactivation of  $S_1$  is responsible for an increased radiationless internal conversion to  $S_0$  in substituted molecules. The reason is that in substituted molecules the planar geometry of  $S_1$  is de-stabilized by the steric repulsion of the side groups, and the excited state energy is partially redistributed on inter-ring motion in  $S_0$ . The  $S_1$ – $S_n$  transition is located at 1.45 eV and decays monomolecularly with 300 ps time constant. The  $S_1$  is a dipole allowed state, even in long  $T_n$  molecules, associated

to strong optical absorption and fairly large emission quantum yield. These characteristics are strongly modified in the solid-state, but in a way that depends on the molecular spatial distribution. In disordered clusters  $S_1$  preserves the molecular character, the  $S_1-S_n$  transition is located around 1.3 eV, but its lifetime is dramatically reduced. The proximity of the molecules leads to a new very efficient non radiative deactivation, tentatively attributed to charge separation [28]. In polycrystalline films, made of a texture of ordered nanocrystals,  $S_1$  bears similarity with that observed in single crystals, the  $S_1-S_n$  transition is further shifted to the red, bi-molecular decay is rather efficient and there is evidence of very weak dipole coupling to  $S_0$ . It is assigned to a Frenkel exciton formed by the original molecular  $S_1$ . In addition to  $S_1$ , either localized or excitonic, the condensed phase support a new excitation, here named the X-state, which apparently does not depend on the molecular spatial arrangement. The X-state is characterized by a PA in the 1.6 eV region, a variable formation time (longer in single crystal) and a long lifetime. It is a sink of energy that control the long time photoexcitation dynamics. Several conjectures have been put forward to explain such state. Being a solid-state effect, it is probably due to the interaction of two or more molecules in a manner different from that of the crystal lattice. Dimer, excimer or CT are similar excitations which may well account for the X-state. We do not know if this state is also connected to photoluminescence, which seems to be due to defects at long times.

## Acknowledgements

We thanks F. Garnier and G. Barbarella for providing us the samples.

## References

- [1] J.W. Sease, L. Zechmeister, *J. Am. Chem. Soc.* 270 (1947) 69.
- [2] F. Garnier, *Acc. Chem. Res.* 32 (1999) 209.
- [3] F. Garnier, G. Horowitz, X. Peng, D. Fichou, *Adv. Mater.* 2 (1990) 592.
- [4] P. Ostoja, S. Guerri, S. Rossini, M. Servidori, C. Taliani, R. Zamboni, *Synth. Met.* 54 (1993) 447.
- [5] A. Dodabalapur, L. Torsi, H.E. Katz, *Science* 268 (1995) 270.
- [6] C. Ziegler, in: H.S. Nalwa (Ed.), *Handbook of Conductive Molecules and Polymers*, Vol. 3, 1997, p. 676.
- [7] C. Ziegler, in: D. Fichou (Ed.), *Handbook of Oligo- and polythiophenes*, Wiley, Weinheim, 1999.
- [8] J.H. Schön, S. Berg, Ch. Kloc, B. Batlogg, *Science* 287 (2000) 1022.
- [9] Ch. Kloc, P.G. Simpkins, T. Siegreist, R.A. Laudise, *J. Crst. Growth* 182 (1997) 416.
- [10] B. Batlogg, Communication at ICSM2000, Badgastein, Austria, 16–21 July 2000.
- [11] F. Garnier, A. Yassar, R. Hajlaoui, G. Horowitz, F. Deloffre, B. Servet, P. Alnot, *J. Am. Chem. Soc.* 115 (1993) 8716.
- [12] G. Barbarella, L. Favaretto, G. Sotgiu, M. Zambianchi, L. Antolini, O. Pudova, A. Bongini, *J. Org. Chem.* 63 (1998) 5497.
- [13] A. Yassar, G. Horowitz, P. Valat, V. Wintgens, M. Kmyene, F. Deloffre, P. Srivastava, P. Lang, F. Garnier, *J. Phys. Chem.* 99 (1995) 9155.
- [14] G. Cerullo, S. Stagira, M. Nisoli, S. De Silvestri, G. Lanzani, G. Kranzelbinder, W. Graupner, G. Leising, *Phys. Rev. B* 57 (1998) 12806.
- [15] G. Lanzani, G. Cerullo, S. stagira, S. De Silvestri, F. Garnier, *J. Chem. Phys.* 111 (1999) 6474.
- [16] F. Charra, D. Fichou, J.-M. Nunzi, N. Pfeffer, *Chem. Phys. Lett.* 192 (1992) 566.
- [17] H. Chosrovian, D. Grebner, S. Rentsch, H. Naarmann, *Synth. Met.* 52 (1992) 213.
- [18] H.-J. Egelhaaf, et al., E-MRS Spring Meeting, Session M-IP20, 1997.
- [19] Y. Kenemitsu, K. Suzuki, Y. Masumoto, Y. Tomiuchi, Y. Shiraishi, M. Kuroda, *Phys. Rev. B* 50 (1994) 2301.
- [20] G. Lanzani, M. Nisoli, S. De Silvestri, R. Tubino, G. Barbarella, M. Zambianchi, *Phys. Rev. B* 51 (1995) 13770.
- [21] G. Lanzani, M. Nisoli, S. De Silvestri, R. Tubino, *Chem. Phys. Lett.* 251 (1996) 339.
- [22] K.S. Wong, H. Wang, G. Lanzani, *Chem. Phys. Lett.* 288 (1998) 59.
- [23] J.-P. Yang, W. Paa, S. Rentsch, *Chem. Phys. Lett.* 320 (2000) 665.
- [24] S. Prandoni, Laurea-thesis, Politecnico di Milano, 1998, unpublished.
- [25] R.S. Becker, J. Seixas de Melo, A.L. Maçanita, F. Elisei, *Pure Appl. Chem.* 67 (1996) 9.
- [26] S.V. Frolov, Ch. Kloc, H. Schön, B. Batlogg, *Phys. Rev. Lett.*, in press.
- [27] G. Klein, *Chem. Phys. Lett.* 320 (2000) 65.
- [28] G. Lanzani, G. Cerullo, S. Stagira, S. De Silvestri, F. Garnier, *Phys. Rev. B* 58 (1998) 7740.
- [29] G. Lanzani, S.V. Frolov, P.A. Lane, Z.V. Vardeny, M. Nisoli, S. De Silvestri, *Phys. Rev. Lett.* 79 (1997) 3066.
- [30] P. Landwehr, H. Port, H.C. Wolf, *Chem. Phys. Lett.* 260 (1996) 125.
- [31] G. Klein, C. Jundt, B. Sipp, A.A. Villaeys, A. Boeglin, A. Yassar, G. Horowitz, F. Garnier, *Chem. Phys. Lett.* 215 (1997) 131.
- [32] C. Zenz, G. Cerullo, G. Lanzani, W. Graupner, F. Meghdadi, G. Leising, S. De Silvestri, *Phys. Rev. B* 59 (1999) 14336.
- [33] R.N. Marks, et al., *Chem. Phys. Lett.* 227 (1998) 49.
- [34] A. Yang, M. Kuroda, Y. Shiraishi, T. Kobayashi, *J. Chem. Phys.* 109 (1998) 8442.
- [35] A.S. Davydov, *Theory of Molecular Excitons*, Plenum Press, New York, 1971.
- [36] M. Kasha, *Radiat. Res.* 20 (1963) 55.
- [37] G. Lanzani, S. Frolov, M. Nisoli, S. De Silvestri, R. Tubino, F. Abbate, P.A. Lane, Z.V. Vardeny, *Synth. Met.* 84 (1997) 517.
- [38] M. Muccini, E. Lunedei, D. Beljonne, J. Cornil, J.L. Bredas, C. Taliani, *J. Chem. Phys.* 23 (1998) 109.
- [39] L. Rossi, G. Lanzani, F. Garnier, *Phys. Rev. B* 58 (1998) 6684.